ISSN 1027-4510, Journal of Surface Investigation: X-ray, Synchrotron and Neutron Techniques, 2020, Vol. 14, Suppl. 1, pp. S56–S59. © Pleiades Publishing, Ltd., 2020.

High-T_C Ferromagnetic Semiconductors: Fake or Fact?

A. Furrer[a, b, *]

[a] *Swiss Neutronics AG, Klingnau, CH-5313 Switzerland*

[b] *Laboratory for Neutron Scattering, Paul Scherrer Institute, Villigen, CH-5232 Switzerland*

**e-mail: albert.furrer@swissneutronics.ch*

Received June 27, 2019; revised July 30, 2019; accepted August 10, 2019

Abstract—The long lasting interest in diluted magnetic semiconductors (DMS) relies on the combination of fundamental science and the potential for spintronics applications. Despite the large body of experimental and theoretical studies carried out in the past decades, there are ongoing controversies about high-T_C ferromagnetic DMS. This paper summarizes the results of the few investigations performed by inelastic neutron scattering, which provides key information for some of the open questions. Emphasis is led on a complete study of the compound $Mn_xGa_{1-x}N$, as well as on novel DMS materials for which the spin injection is decoupled from carrier doping.

Keywords: diluted magnetic semiconductors, exchange interaction, inelastic neutron scattering

DOI: 10.1134/S1027451020070150

INTRODUCTION

Traditional semiconductors are based on the control of charge carriers (*n*- or *p*-type). Magnetic-ion-doped semiconductors allow, in addition, the control of the quantum spin state (up or down), which have attracted great interest because of their potential applications in spintronics and blue-light emitting diode (LED) technologies [1, 2]. The main challenge for practical applications is the attainment of a Curie temperature T_C above room temperature to be compatible with junction temperatures. So far, the highest Curie temperatures were obtained for $Mn_xGa_{1-x}As$ ($x = 0.13$) with $T_C = 190$ K [3], as well as for $(K_xBa_{1-x})(Mn_yZn_{1-y})_2As_2$ ($x = 0.3$, $y = 0.15$) with $T_C = 230$ K [4]. The observation of ferromagnetism above room temperature reported by several authors has to be considered with caution, as these findings neither resulted in a device working at room temperature nor were confirmed by other groups.

Here we discuss how neutron scattering experiments can contribute to resolve the ongoing controversies about high-T_C ferromagnetic semiconductors. The problems to be addressed are fourfold: (i) What is the solubility limit of the doped magnetic ions in the host compound? (ii) Where are the doped magnetic ions located in the host compound? (iii) What is the valence of the doped magnetic ions? (iv) What is the doping-induced enhancement of the ferromagnetic exchange interaction? The present paper provides answers to these questions by summarizing the few inelastic neutron scattering experiments performed for diluted magnetic semiconductors (DMS) in the past.

STRATEGY OF INELASTIC NEUTRON SCATTERING EXPERIMENTS ON DMS

The content of magnetic ions in DMS compounds is rather low, thus, the magnetic excitations can be associated with monomers and dimers resulting from the random distribution of the magnetic ions. The spin Hamiltonian of magnetic dimers is given by

$$H_D = -2J\mathbf{s}_1 \cdot \mathbf{s}_2, \quad (1)$$

where J is the bilinear exchange parameter and $\mathbf{s}_i$ is the spin operator of the magnetic ions. It is convenient to base the diagonalization of (1) on the dimer states $|S, M\rangle$, where $\mathbf{S} = \mathbf{s}_1 + \mathbf{s}_2$ is the total spin and $-S \le M \le S$. For magnetic ions with $s_i = 1/2$, ferromagnetic ($J > 0$) and antiferromagnetic ($J < 0$) exchanges give rise to an $S = 1$ triplet and an $S = 0$ singlet ground-state, respectively. The energy separation E_D between the singlet and triplet states is $2J$, which can be directly measured by inelastic neutron scattering experiments. When the magnetic ions experience single-ion anisotropy, Eq. (1) should be extended by the Hamiltonian

$$H_M = D(s_z)^2 \quad (2)$$

for the case of axial anisotropy. Monomer excitations are governed by (2).

The doped magnetic ions inject charge carriers into the host compound which are expected to generate a sizable ferromagnetic component to the exchange interaction through Zener's kinetic exchange mechanism [5]:

$$H_{\text{Zener}} = J_H \Sigma_i \boldsymbol{\sigma} \cdot \mathbf{s}_i, \quad (3)$$

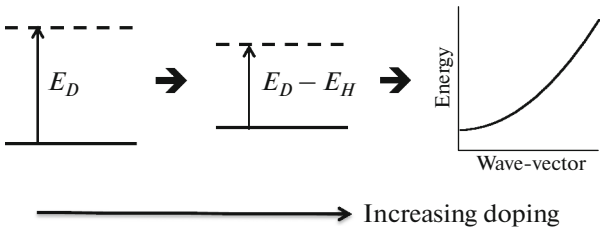

Fig. 1. Schematic picture illustrating the decrease in the singlet-triplet splitting and the turnover into collective magnetic excitations with increasing doping.

where $\boldsymbol{\sigma}$ is the spin operator of the charge carriers and J_H is the local exchange (Hund's coupling) parameter. This mechanism favors a ferromagnetic alignment between the charge carriers and the magnetic ions. If the dimer ground state is a singlet, the application of (3) produces a spin flip of one of the magnetic ions, reducing the singlet-triplet splitting by [6]

$$E_H = t_{\text{eff}} S/(2s_i + 1), \qquad (4)$$

where $t_{\text{eff}} \ll J_H$ is the hopping parameter. The successive decrease in the singlet-triplet splitting E_D with increasing E_H is schematically shown in Fig. 1. For sufficiently large values of E_H, the magnetic response turns into a collective magnetic excitation, which can coexist with dimer excitations [7].

MATERIALS INVOLVING CO-DOPING OF CHARGE AND SPIN

Doping with transition-metal ions produces both magnetic moments and charge carriers in the host compound. Up to the present, the inelastic neutron scattering investigations focused on pnictide and chalcogenide systems. The first inelastic neutron scattering experiments were performed for $Co_{0.05}Mg_{0.95}O$ [8] with the aim to search for light permanent magnets. The observed energy spectra revealed the presence of both ferromagnetic and antiferromagnetic dimer couplings (Fig. 2). The data interpretation was later confirmed by a study of the magnetic excitations in CoO [9]. The compound MgO is a perfect insulator with a band gap of 7.8 eV, but very recently it was shown that doping by transition-metal ions decreased the band gap down to 2.8 eV [10], making $Co_xMg_{1-x}O$ a new and promising DMS candidate.

The second inelastic neutron scattering experimental series were carried out for $Mn_xZn_{1-x}Te$ [11]. Mn doping with $x = 0.05$ produced a downward shift of the dimer splittings, thereby proving the expectations illustrated in Fig. 1. However, the downward shift amounted only to a few percent, since the number of mobile charge carriers (holes) produced by Mn doping is rather small; thus, $Mn_xZn_{1-x}Te$ cannot be considered as a useful DMS candidate.

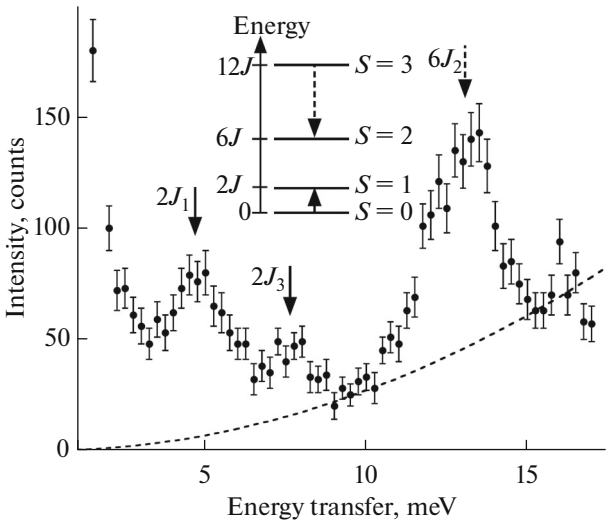

Fig. 2. Energy spectrum of neutrons observed for $Co_{0.05}Mg_{0.95}O$ at $T = 12$ K and modulus of the scattering vector $Q = 1.4$ Å^{-1}. The dashed line corresponds to the phonon scattering. The full and dashed arrows mark the observed dimer transitions involving antiferromagnetic and ferromagnetic exchange interactions J_i, respectively, with the assignments shown in the inset. Exchange interactions J_1, J_2, and J_3 refer to nearest-neighbor, next-nearest-neighbor and third-nearest-neighbor pairs of Co^{2+} ions, respectively.

The third inelastic neutron scattering experiments concerned $Mn_xGa_{1-x}N$, which aroused great interest driven by the prediction of Mn-induced ferromagnetism with Curie temperatures T_C exceeding room temperature [12]. In spite of a large number of experimental studies, the conclusions remained highly controversial, as summarized by Nelson et al. [13]. A basic problem is the solubility of Mn ions in the host compound GaN, so that the investigated samples are often contaminated by Mn clusters or other phases which are ferromagnetic in nature, e.g., $Mn_{3-x}Ga$ ($T_C = 770$ K) and Mn_4N ($T_C = 738$ K). For this reason, the observation of ferromagnetism above room temperature remains unsubstantiated. Recently, an experimental study was initiated for $Mn_xGa_{1-x}N$ [14] in order to address the existing controversial issues. Polycrystalline samples were synthesized for $x = 0.02$ and 0.04 and analyzed by X-ray and neutron diffraction, showing little contamination by MnN_y ($y < 1$). The doped Mn ions enter the host lattice close to the Ga sites with a displacement of about 0.3 Å along the z-direction. X-ray absorption near-edge structure (XANES) experiments confirmed the divalent nature of the Mn ions, so that the replacement of Ga^{3+} ions by Mn^{2+} ions creates holes in the system. The energy spectra observed in inelastic neutron scattering experiments for $x = 0.04$ revealed three partially resolved lines (Fig. 3a), which shows the intensity difference between $T = 6$ and 1.7 K, so that uncertainties about

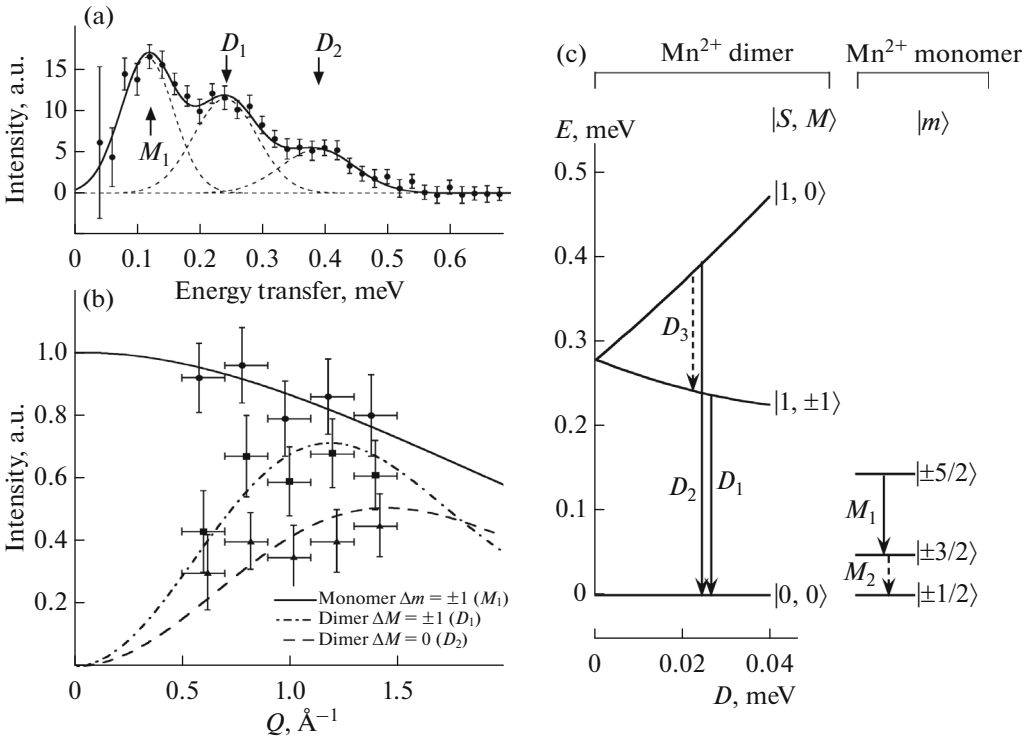

Fig. 3. (a) Energy spectrum of neutrons scattered from $Mn_{0.04}Ga_{0.96}N$ for moduli of the scattering vector **Q** in the range $0.5 \le Q \le 1.5$ Å^{-1}. The data correspond to the intensity difference $I(T = 6.0\text{ K}) - I(T = 1.7\text{ K})$. The lines are the result of a Gaussian least-squares fit. The arrows denote the monomer (M_i) and dimer (D_i) transitions. (b) Q-dependence of the neutron cross-section for Mn^{2+} monomers and dimers. The lines correspond to the calculated intensities, and the circles, squares, and triangles to the intensities observed for the transitions M_1, D_1 and D_2, respectively. (c) Energy level splittings of Mn^{2+} monomers and dimers in $Mn_{0.04}Ga_{0.96}N$. The full arrows mark the observed transitions displayed in Fig. 3a. The dashed arrows refer to the remaining allowed transitions not observed in the inelastic neutron scattering experiments (the transition M_1 could not be resolved from the elastic line, and the transition matrix element of D_3 is an order of magnitude smaller than for D_1 and D_2).

the background scattering are automatically eliminated. The three lines correspond to Mn^{2+} monomer (M_i) and dimer (D_i) excitations, which could be distinguished from each other by considering the Q-dependence of the intensities [15] (Fig. 3b). The low-energy level schemes for Mn^{2+} monomers and dimers are shown in Fig. 3c, from which the parameters $D = 0.029(3)$ meV and $J = -0.140(7)$ meV can be extracted. The inelastic neutron scattering data obtained for $x = 0.02$ turned out to be very similar (but with smaller intensity) to those displayed in Fig. 3a. The independence of the antiferromagnetic exchange parameter J on the Mn content x means that the injected holes are localized to a large extent, so that they cannot generate a sizable ferromagnetic component. In fact, the concentration of mobile holes was measured to be $<10^{18}$ cm^{-3} for crystalline $Mn_xGa_{1-x}N$ ($x < 0.1$) [16]. In view of all these facts, it can be concluded that the ferromagnetism reported in the literature for $Mn_xGa_{1-x}N$ is likely due to the presence of ferromagnetic impurity phases.

MATERIALS DECOUPLING CARRIER DOPING FROM SPIN INJECTION

During the last 5–10 years, novel DMS materials have been discovered, namely $Li_{1-x}(Mn_yZn_{1-y})As$ [17] and $(K_xBa_{1-x})(Mn_yZn_{1-y})As_2$ [4], for which carrier doping is decoupled from the spin injection. Heterovalent carrier doping (x) and spin injection by isovalent substitution (y) occur in different crystallographic planes, which is highly beneficial to avoid the solubility problem addressed in the introduction. The first inelastic neutron scattering experiments on these novel DMS systems were recently reported for $(K_xBa_{1-x})(Mn_yZn_{1-y})As_2$ with $x = 0.2$ and $y = 0.15$ [6]. The undoped compound ($x = 0$) shows a well resolved peak at 14 meV corresponding to the singlet-triplet splitting of antiferromagnetically coupled Mn^{2+} dimers. For the doped compound ($x = 0.2$), the peak is shifted downwards to 13 meV and the linewidth is doubled. The authors of [6] argue that this observation is associated with the destruction of the Mn singlet ground-state, since the As bands become metallic and

spin polarized upon doping and, thus, generate a Stoner continuum in the excitation spectrum.

CONCLUSIONS

The history of DMS materials involving co-doping of charge and spin started in 1996 with the compound $Mn_xGa_{1-x}As$ ($x = 0.035$) exhibiting $T_C = 60$ K [18]. The Curie temperature was subsequently increased and reached a maximum of $T_C = 190$ K for $x = 0.13$ in 2013 [3]. Since then, no further increase in T_C has been reported. Obviously, the most promising route is offered by DMS materials where charge and spin doping are decoupled: it took only 3 years to raise the Curie temperature up from $T_C = 50$ K in 2011 [17] to 230 K in 2014 [4]. There is no reason to believe that this development has already leveled off. What is needed is a deepening of the understanding of the doping mechanism, for which an enhancement of inelastic neutron scattering studies on single crystals are highly desirable.

ACKNOWLEDGMENTS

The author is grateful to K.W. Krämer (University of Berne), A. Podlesnyak (Oak Ridge National Laboratory), as well as V. Pomjakushin, D. Sheptyakov, and O.V. Safonova (PSI Villigen) for their expert co-operation in the course of the experimental studies.

REFERENCES

1. I. Zutic, J. Fabian, and S. D. Sarma, Rev. Mod. Phys. **76**, 323 (2004). https://doi.org/10.1103/RevModPhys.76.323
2. H. Amano, N. Sawacki, I. Akasaki, and Y. Toyoda, Appl. Phys. Lett. **48**, 353 (1986).
3. P. Nemec et al., Nat. Commun. **4**, 1422 (2013). https://doi.org/10.1038/ncomms2426
4. K. Zhao, B. Chen, G. Zhao, Z. Yuan, Q. Liu, Z. Deng, J. Zhu, and C. Jin, Chin. Sci. Bull. **59**, 2524 (2014). https://doi.org/10.1007/s11434-014-0398-z
5. C. Zener, Phys. Rev. **81**, 440 (1951).
6. M. A. Surmach, B. J. Chen, Z. Deng, C. Q. Jin, J. K. Glasbrenner, I. I. Mazin, A. Ivanov, and D. S. Inosov, Phys. Rev. B **97**, 104418 (2018). https://doi.org/10.1103/PhysRevB.97.104418
7. A. Furrer and H. U. Güdel, Eur. Phys. J. B **16**, 81 (2000).
8. V. Wagner and A. Furrer, *Report AF-SSP-113* (ETH, Zurich, 1980).
9. K. Tomiyasu and S. Itoh, J. Phys. Soc. Jpn. **75**, 084708 (2006). https://doi.org/10.1143/JPSJ.75.084708
10. M. M. Obeid, S. J. Edrees, and M. M. Shukur, Superlattices Microstruct. **122**, 124 (2018). https://doi.org/10.1016/j.spmi.2018.08.015
11. H. Kepa, L. Van Khoi, C. M. Brown, M. Sawicki, J. K. Furdyna, T. M. Giebultowicz, and T. Dietl, Phys. Rev. Lett. **91**, 087205 (2003). https://doi.org/10.1103/PhysRevLett.91.087205
12. T. Dietl, H. Ohno, and F. Matsukara, Phys. Rev. B: Condens. Matter Mater. Phys. **63**, 195205 (2001). https://doi.org/10.1103/PhysRevB.63.195205
13. R. Nelson, T. Berlijn, J. Moreno, M. Jarrell, and W. Ku, Phys. Rev. Lett. **115**, 197203 (2015). https://doi.org/10.1103/PhysRevLett.115.197203
14. A. Furrer, K. W. Krämer, A. Podlesnyak, V. Pomjakushin, D. Sheptyakov, and O. V. Safonova, Phys. Rev. B **97**, 140102(R) (2018). https://doi.org/10.1103/PhysRevB.97.140102
15. A. Furrer and O. Waldmann, Rev. Mod. Phys. **85**, 367 (2013). https://doi.org/10.1103/RevModPhys.85.367
16. M. Zajac, R. Doradziński, J. Gosk, et al., Appl. Phys. Lett. **78**, 1276 (2001). https://doi.org/10.1063/1.1348302
17. Z. Deng, C. Q. Jin, Q. Q. Liu, et al., Nat. Commun. **2**, 422 (2011). https://doi.org/10.1038/ncomms1425
18. H. Ohno, A. Shen, F. Matsukara, A. Oiwa, A. Endo, S. Katsumoto, and Y. Iye, Appl. Phys. Lett. **69**, 363 (1996).